FEBS Letters 446 (1999) 264–268 FEBS 21686

# Unique topology of the internal repeats in the cardiac $Na^+/Ca^{2+}$ exchanger

Takahiro Iwamoto[a], Tomoe Y. Nakamura[a], Yan Pan[a], Akira Uehara[b], Issei Imanaga[b], Munekazu Shigekawa[a,*]

[a] *Department of Molecular Physiology, National Cardiovascular Center Research Institute, Suita, Osaka 565-8565, Japan*
[b] *Department of Physiology, School of Medicine, Fukuoka University, Fukuoka 814-0180, Japan*

Received 28 December 1998; received in revised form 29 January 1999

**Abstract Hydropathy analysis predicts 11 transmembrane helices in the cardiac $Na^+/Ca^{2+}$ exchanger. Using cysteine susceptibility analysis and epitope tagging, we here studied the membrane topology of the exchanger, in particular of the highly conserved internal α-1 and α-2 repeats. Unexpectedly, we found that the connecting loop in the α-1 repeat forms a re-entrant membrane loop with both ends facing the extracellular side and one residue (Asn-125) being accessible from the inside and that the region containing the α-2 repeat is mostly accessible from the cytoplasm. Together with other data, we propose that the exchanger may consist of nine transmembrane helices.**



*Key words:* $Na^+/Ca^{2+}$ exchanger; Membrane topology; Cysteine susceptibility analysis; Epitope tagging

## 1. Introduction

The plasma membrane $Na^+/Ca^{2+}$ exchanger is an electrogenic transporter that catalyzes the exchange of three $Na^+$ for one $Ca^{2+}$. It is involved primarily in the extrusion of $Ca^{2+}$ from the cytoplasm, although it may mediate $Ca^{2+}$ influx under some conditions. The mammalian $Na^+/Ca^{2+}$ exchanger forms a multigene family of three isoforms NCX1, NCX2 and NCX3, which share ~70% identity in overall amino acid sequences [1–3]. On the basis of the hydropathy analysis, the mature exchanger protein is modeled to consist of 11 transmembrane helices (TMs) and a large central hydrophilic loop between TM5 and TM6 [4]. Interestingly, $Na^+/Ca^{2+}$ exchange occurs almost normally in a mutant exchanger deleted for the large central loop, indicating that the transmembrane domain alone is sufficient to catalyze ion transport [5,6]. The large central loop is involved in the regulation of the exchanger by intracellular cations [7], phosphatidylinositol 4,5-bisphosphate [8] and protein phosphorylation [6,9]. Thus, this loop is exposed on the cytoplasm.

Recent studies have provided evidence that the N-terminus of the exchanger is localized on the extracellular side of the plasma membrane, while the C-terminus and the loop connecting TM1-TM2 are exposed to the cytoplasm [10,11]. Strikingly, all members of the $Na^+/Ca^{2+}$ exchanger family and the $Na^+/Ca^{2+}/K^+$ exchangers have highly conserved internal repeat sequences designated the α-1 and α-2 repeats [4,12], which are modeled to comprise most of the sequences in TM2-TM3 and TM8-TM9 and the loops connecting these transmembrane helices (see Fig. 3A). Mutation of amino acid residues within the putative transmembrane helices of α-1 and α-2 repeats results in a large reduction of the exchange activity or a change in the I-V relationship in NCX1 [4], suggesting the functional importance of these conserved regions. At present, however, little is known about the structure/function relationship in the transmembrane domain of the exchanger molecule.

In this study, using cysteine susceptibility analysis [13] and c-myc epitope tagging, we studied the membrane topology of the NCX1 polypeptide, with a particular focus on the internal α-1 and α-2 repeats. We here provide evidence that the connecting loop in the α-1 repeat forms a pore loop-like structure, whereas the α-2 repeat region may form a domain exposed on the cytoplasmic surface. Our data suggest that the exchanger is comprized of nine TMs. This novel information on the exchanger topology will give a new insight into the structural basis of the exchanger function.

## 2. Materials and methods

### 2.1. Cell cultures

CCL39 cells (American Type Culture Collection) and NCX1 transfectants were maintained in Dulbecco's modified Eagle's medium supplemented with 7.5% heat-inactivated fetal calf serum, 50 U/ml penicillin and 50 μg/ml streptomycin.

### 2.2. Construction and stable expression of cysteine-substituted or epitope-tagged NCX1

cDNA of dog heart NCX1.1 was cloned into the mammalian expression vector pKCRH using *Sac*II-*Hin*dIII sites (designated pKCRH-NCX1) [9]. Substitution of each amino acid residue by cysteine and insertion of an epitope peptide sequence were achieved by site-directed mutagenesis as described [6]. Briefly, two DNA fragments were produced by PCR using *Pfu* polymerase and two pairs of outer and inner primers, with inner primers containing an overlapping sequence with the same desired mutation or with an additional epitope peptide sequence. The final PCR products were generated with these DNA fragments as templates using two outer primers. For mutations in amino acids 1–530, the primers corresponding to a 5′ non-coding region (sense) and nucleotides 1730–1750 (antisense) were used, whereas for mutation in amino acids 534–938 the primers corresponding to nucleotides 1690–1710 (sense) and a 3′ non-coding region (antisense) were used. After digestion with restriction enzymes, the final PCR products were inserted into pKCRH-NCX1. For the construction of epitope-tagged exchangers, the human c-myc epitope (EQKLISEEDLN) was inserted between Pro-31 and Gln-32 in the N-terminal portion or between Phe-938 and the stop codon in the C-terminal portion (designated Myc-NT or Myc-CT, respectively). Successful construction was verified by sequencing (ABI PRISM, Perkin-Elmer). pKCRH plasmids were transfected into CCL39 cells using Lipofectin (Gibco BRL) and stable cell clones exhibiting high $Na^+/Ca^{2+}$ exchange activity were selected by ionomycin treatment ($Ca^{2+}$ killing) [14].

*Corresponding author. Fax: (81) (6) 6872-7485.
E-mail: shigekaw@ri.ncvc.go.jp


PII: S0014-5793(99)00218-5

*2.3. Assay of intracellular $Na^+$ ($Na^+_i$)-dependent $^{45}Ca^{2+}$ uptake*

For cell $Na^+$ loading, confluent cells in 24 well dishes were incubated at 37°C for 30 min in 0.5 ml of BSS (146 mM NaCl, 4 mM KCl, 2 mM $MgCl_2$, 0.1 mM $CaCl_2$, 10 mM glucose and 10 mM HEPES/Tris (pH 7.4)) containing 1 mM ouabain and 10 μM monensin. Cells were treated with 10 mM membrane impermeant SH labelling reagent (2-(trimethylammonium)ethyl)methanethiosulfonate bromide (MTSET) (Toronto Research Chemicals) during the last 10 min of cell $Na^+$ loading and then washed three times. The rate of $Na^+_i$-dependent $^{45}Ca^{2+}$ uptake into cells was measured for 30 s as described previously [15]. The rate of uptake into cells pretreated with MTSET was normalized to that into untreated control cells and expressed as percentage of the latter (Fig. 1).

*2.4. Measurement of whole cell exchange currents*

Exchange currents from transfectants were measured using the whole cell voltage clamp technique as described [16]. Outward and inward currents were elicited employing a standard square step voltage protocol [17], in which membranes were depolarized from a holding potential of −30 mV to +60 mV for 500 ms followed by hyperpolarization to −80 mV for 500 ms. This protocol was repeated at every 20 s for 6–10 min. The bath solution contained 140 mM Na glutamate, 1 mM $MgCl_2$, 1.8 mM $CaCl_2$, 0 or 5 mM $NiSO_4$, 20 μM ouabain, 2 μM verapamil, 0 or 1 mM MTSET and 5 mM HEPES (pH 7.4). The pipette solution contained 120 mM CsOH, 6 mM $MgCl_2$, 7 mM $CaCl_2$, 5 mM $Na_2ATP$, 50 mM aspartic acid, 5 mM creatine phosphate, 20 mM EGTA, 20 mM tetraethylammonium chloride, 0 or 10 mM MTSET and 20 mM HEPES (pH 7.2). Control and MTSET inhibitable exchange currents were estimated as $Ni^{2+}$-sensitive charge movements that were quantified by integrating $Ni^{2+}$-sensitive outward currents recorded with or without MTSET. The $Ni^{2+}$-sensitive current was never observed in non-transfected cells (data not shown). Control and MTSET-blocked outward currents were measured in the same cell. To examine the effect of internally applied MTSET, the control current was monitored initially within 15 s after rupturing the cell membrane and then the MTSET-blocked current was monitored after the current reached a steady state in ~6 min. $Ni^{2+}$ was subsequently applied to the bath to estimate the $Ni^{2+}$-insensitive charge movement, which was subtracted from the control or MTSET-blocked one. For the effect of externally applied MTSET, the exchange current was measured before or ~6 min after placing cells in a bath solution containing 1 mM MTSET. The $Ni^{2+}$-sensitive charge movement measured with MTSET was normalized to the $Ni^{2+}$-sensitive control charge movement and expressed as percentage of the latter (Fig. 1). As the time-matched control, we performed similar experiments without MTSET in the pipette or bath solution. We found no significant change in the currents using this protocol. All experiments were performed at about 34°C. Data were acquired and analyzed by the pCLAMP (Axon Instrument) software.

*2.5. Immunofluorescence*

For permeabilization, cells were fixed in BSS containing 4% paraformaldehyde for 5 min at 25°C and then permeabilized in BSS containing 0.5% Triton X-100 for 5 min at 25°C. Intact cells and permeabilized cells were incubated with anti-c-myc monoclonal antibody (9E10, Genosys) (1:50) for 0.5 h at 37°C and 3 h at 25°C, respectively, in BSS containing 5% BSA. These cells were subsequently washed five times with the same medium and then treated with FITC-conjugated donkey anti-mouse IgG (Cappel) (1:500). After three washes, cells were observed by confocal laser scanning microscopy using a Bio-Rad MRC-1024 system mounted on an Olympus BX50WI microscope with a plan-apochromat ×40 water immersion lens.

*2.6. Statistical analysis*

Data are expressed as means ± S.E. of three–seven independent determinations. Differences were analyzed by unpaired *t*-test. Values of $P < 0.05$ were considered statistically significant.

## 3. Results and discussion

On the basis of the hydropathy analysis and available experimental evidence, the mature $Na^+/Ca^{2+}$ exchanger protein has been predicted to consist of 11 TMs with the C-terminus and the large central hydrophilic loop localized on the intracellular side of the membrane and the N-terminus being on the extracellular side (see Section 1). Hence, five and six TMs are predicted to separate the N-terminus and the large central loop, and the large central loop and the C-terminus, respectively [4] (see Fig. 3A, 11 TM model).

In this study, we investigated the membrane topology of the cardiac $Na^+/Ca^{2+}$ exchanger expressed in CCL39 fibroblasts that are devoid of endogenous exchange activity [6,9,14]. To determine the validity of the 11 TM model, in particular the topology of the α-1 and α-2 repeat regions, we selected amino acid residues that are predicted by this model to be near the surface of the membrane and on the loops connecting TM2-TM3 and TM8-TM9 and examined their intracellular or extracellular accessibility using cysteine susceptibility analysis [13]. In this analysis, targeted residues were individually mutated to cysteine and the inhibition of exchange activity of the resulting mutants by membrane impermeant SH labelling reagent MTSET was assessed. MTSET and its related compounds form an irreversible, covalent bond with the sulfhydryl group in cysteine and have been used successfully in identifying residues accessible from extracellular and intracellular media in channels and transporters [10,13,18,19].

To assess the accessibility by externally applied MTSET, we measured the rate of $Na^+_i$-dependent $^{45}Ca^{2+}$ uptake into CCL39 cells expressing cysteine-substituted mutants in the presence and absence of MTSET. On the other hand, the accessibility by intracellular MTSET was assessed by measuring the whole cell outward exchange currents from single cells expressing cysteine-substituted mutants. The activity of each cysteine-substituted mutant used in this study is shown in Fig. 1 (see relative activity). Some mutants displayed a low uptake activity, which probably results from a reduced exchange activity or reduced synthesis of the mutated proteins.

We found that extracellular or intracellular application of MTSET exerted little effect on the activity of the wild-type exchanger (Fig. 1), although the mature exchanger protein contains 15 endogenous cysteine residues. This result is consistent with the previous observation [10]. On the other hand, the Leu-102 to Cys mutant (L102C) was inhibited by intracellular but not by extracellular MTSET (Fig. 1), indicating the intracellular accessibility of this residue. In contrast, E120C was inhibited by extracellular but not by intracellular MTSET. The intervening residues Leu-107 and Ser-117 were inhibited neither by intracellular nor extracellular MTSET. On the other hand, I136C was inhibited only by extracellular MTSET, whereas V155C and R161C were inhibited only by intracellular MTSET. These results are consistent with the 11 TM model which predicts that Leu-102 is localized at the N-terminal end of TM2, that Leu-107 and Ser-117 are localized within TM2 and that Ile-136, Val-155 and Arg-161 are localized at the extracellular and cytoplasmic side of TM3, respectively.

We further examined the accessibility of residues in the loop connecting TM2-TM3. We found that G123C, A128C, G129C and S134C were inhibited by extracellular MTSET, indicating that these residues are accessible from the extracellular side (Fig. 1). Ileu-136 at the end of this loop was also inhibited by extracellular MTSET as described above. Unexpectedly, however, N125C was inhibited by intracellular but not by extracellular MTSET. As for the mutants H124C, T127C and D130C, we did not observe statistically significant inhibition by either intracellular or extracellular MTSET. We

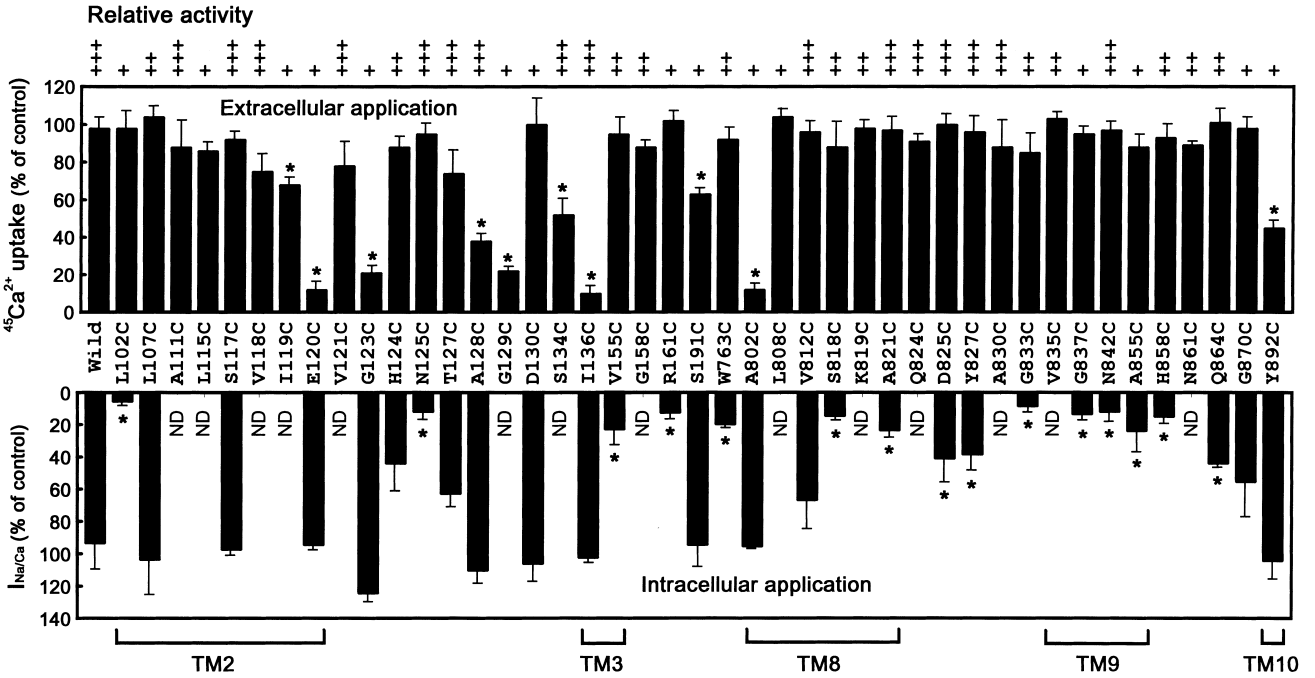


Fig. 1. Effect of extracellular or intracellular application of MTSET on activities of the wild-type or cysteine-substituted exchangers. The upper panel shows the effect of extracellular MTSET on the rate of $Na^+_i$-dependent $^{45}Ca^{2+}$ uptake measured as described in Section 2.3. The lower panel shows the effect of intracellular MTSET on the whole cell outward exchange currents measured from three–seven single transfectants as detailed in Section 2.4. The columns marked with an asterisk are significantly different ($P < 0.05$) from those for the wild-type transfectants. ND, not determined. Relative activity, uptake activities of transfectant clones are shown: +, 0.5∼1 nmol/mg/30 s; ++, 1∼3 nmol/mg/30 s; +++, 3∼8 nmol/mg/30 s.

also examined the accessibility of residues in TM8-TM9 and the loop connecting these putative transmembrane helices. A802C was inhibited by extracellular but not by intracellular MTSET (Fig. 1). In contrast, S818C, A821C, D825C, Y827C, G833C, G837C, N842C and A855C were all inhibited by intracellular but not by extracellular MTSET. Other mutants L808C, K819C, Q824C, A830C and V835C were not affected by extracellular MTSET.

We assessed the accessibility of G123C, N125C, A128C and G833C in the loops connecting TM2-3 and TM8-9 by examining the effect of extracellular MTSET on the whole cell outward exchange currents from single cells expressing these mutants. The exchange currents from wild-type, G123C, N125C, A128C and G833C in the presence of extracellular MTSET were 100 ± 18, 8.8 ± 13*, 116 ± 24, 4.0 ± 1.3* and 135 ± 19% of the controls measured in the absence of the reagent, respectively ($n$=3 or 4; *$P < 0.05$ versus the wild-type). Thus, we confirmed the results obtained from $^{45}Ca^{2+}$ uptake measurements with these mutants (Fig. 1). These data, together with those described in the preceding paragraph, suggest that the

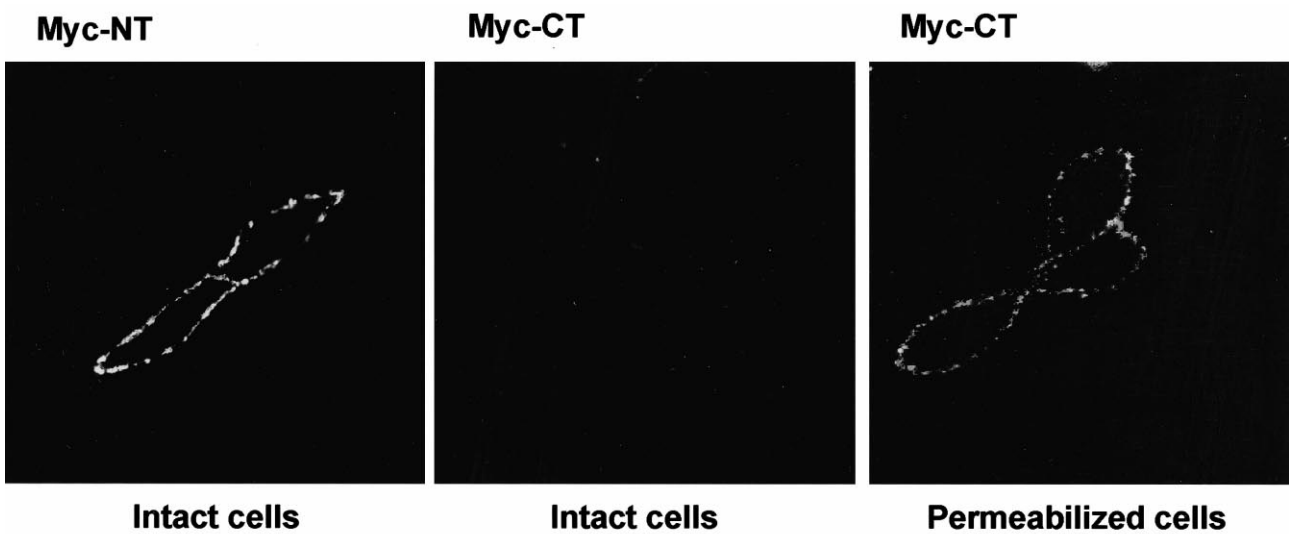


Fig. 2. Immunofluorescent staining of cells expressing c-myc epitope-tagged exchangers. Intact cells expressing Myc-NT or Myc-CT and permeabilized cells expressing Myc-CT were stained with anti-c-myc antibody 9E10.

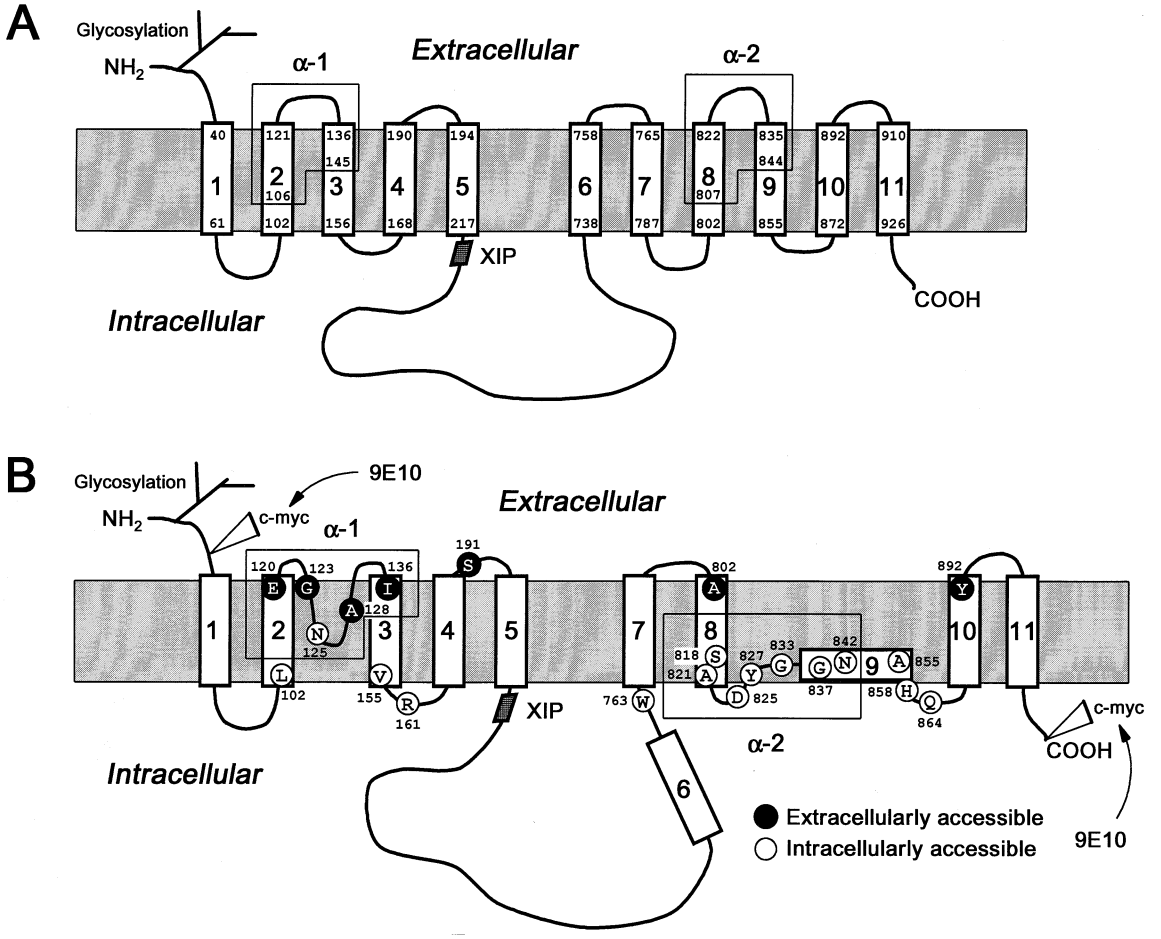


Fig. 3. Topological models of the $Na^+/Ca^{2+}$ exchanger. A: original 11 TM model. B: new model. The results of cysteine susceptibility analysis are shown: closed circles, residues accessible only to extracellular MTSET; open circles, residues accessible only to intracellular MTSET. The positions of c-myc epitope tag are indicated by an open triangle. Open boxes with Arabic numbers are the transmembrane helices previously modeled on the basis of hydropathy analysis. XIP, exchanger inhibitory peptide region.

loop connecting TM2-TM3 forms a re-entrant membrane loop with both ends facing the extracellular side and Asn-125 being accessible from the intracellular side (see new model in Fig. 3B). In contrast, the portion of the exchanger containing the putative TM8-TM9 and the loop connecting them are mostly accessible from the cytoplasmic side.

We further examined the location of other putative loops. S191C and Y892C were modestly, but significantly, inhibited by extracellular MTSET, whereas W763C was sensitive to inhibition only by intracellular MTSET (Fig. 1). H858C and Q864C were also inhibited only by intracellular MTSET. These data are consistent with the view that the loop connecting TM4-TM5 in the 11 TM model is accessible from the extracellular side, while the putative loops connecting TM6-TM7 and TM9-TM10 are accessible from the cytoplasmic side. Furthermore, the region immediately C-terminal to TM10 seems to be located on the extracellular surface.

We assessed the accessibility of the human c-myc epitope introduced into the N-terminus (Myc-NT) or the C-terminus (Myc-CT) of the exchanger molecule. Both tagged mutants expressed in CCL39 cells exhibited high exchange activities equivalent to that of the wild-type exchanger (data not shown). As shown in Fig. 2, Myc-NT was stained with anti-c-myc antibody 9E10 in intact cells, whereas Myc-CT was detected with the antibody only in permeabilized cells, indicating that the N-terminal and C-terminal portions of the exchanger are localized on the extracellular and cytoplasmic surfaces of the membrasne, respectively. This finding is consistent with the previous report [11].

Based on the results described in the preceding paragraphs, we propose a new topological model of the exchanger molecule consisting of nine TMs as illustrated in Fig. 3B. In marked contrast to the 11 TM model, the region encompassing Ser-818–Asn-842, which contains most of the α-2 repeat, is placed on the cytoplasmic side. Unfortunately, however, the current data alone are not sufficient to delineate the structure of this region. TM6 is also placed on the cytoplasmic side, because hydrophobicity of this segment is significantly less than those of other TMs and because some algorithms for prediction of transmembrane helices and topology predict it to be intracellular [11].

Our prediction of topology of the N-terminal half of the transmembrane domain of the exchanger is similar to that of the 11 TM model, except that the connecting loop in the α-1 repeat forms a re-entrant membrane loop with both ends facing the extracellular side and one of the residue (Asn-125) being readily accessible from the cytoplasm (Fig. 3B). This latter structure is reminiscent of pore loops from ion channels

[20]. The glutamate transporter GLT-1 also has a pore loop-like structure, although the function of this loop is not known [19]. Recently we have obtained an important clue to the function of this pore loop-like structure in the $Na^+/Ca^{2+}$ exchanger. We have observed that the divalent cation $Ni^{2+}$, a competitive inhibitor of transport substrate $Ca^{2+}$, is 10-fold more inhibitory to NCX1 than to NCX3 [15]. Using chimeras between NCX1 and NCX3 and site-directed mutagenesis, Asn-125 and Thr-127 within the loop of the α-1 repeat were found to be partly responsible for the observed differential responses of NCX isoforms to $Ni^{2+}$ (T. Iwamoto et al., unpublished observation). Thus, the re-entrant loop in the α-1 repeat could be an important structure involved in the binding and transport of substrate cations.

*Acknowledgements:* This work was supported by Grant-in-Aid for Priority Areas (09273101) and Encouragement of Young Scientists (10770048) from the Ministry of Education, Science and Culture of Japan and a grant from the Human Science Research Foundation.

## References

[1] Nicoll, D.A., Longoni, S. and Philipson, K.D. (1990) Science 250, 562–565.
[2] Li, Z., Matsuoka, S., Hryshko, L.V., Nicoll, D.A., Bersohn, M.M., Burke, E.P., Lifton, R.P. and Philipson, K.D. (1994) J. Biol. Chem. 269, 17434–17439.
[3] Nicoll, D.A., Quednau, B.D., Qui, Z., Xia, Y.-R., Lusis, A.J. and Philipson, K.D. (1996) J. Biol. Chem. 271, 24914–24921.
[4] Nicoll, D.A., Hryshko, L.V., Matsuoka, S., Frank, J.S. and Philipson, K.D. (1996) J. Biol. Chem. 271, 13385–13391.
[5] Matsuoka, S., Nicoll, D.A., Reilly, R.F., Hilgeman, D.W. and Philipson, K.D. (1993) Proc. Natl. Acad. Sci. USA 90, 3870–3874.
[6] Iwamoto, T., Pan, Y., Nakamura, T.Y., Wakabayashi, S. and Shigekawa, M. (1998) Biochemistry 37, 17230–17238.
[7] Hilgemann, D.W. (1996) Ann. New York Acad. Sci. 779, 136–158.
[8] Hilgemann, D.W. and Ball, R. (1996) Science 273, 956–959.
[9] Iwamoto, T., Pan, Y., Wakabayashi, S., Imagawa, T., Yamanaka, H.I. and Shigekawa, M. (1996) J. Biol. Chem. 271, 13609–13615.
[10] Doering, A.E., Nicoll, D.A., Lu, Y., Lu, L., Weiss, J.N. and Philipson, K.D. (1998) J. Biol. Chem. 273, 778–783.
[11] Cook, O., Low, W. and Rahamimoff, H. (1988) Biochim. Biophys. Acta 1371, 40–52.
[12] Schwarz, E.M. and Benzer, S. (1997) Proc. Natl. Acad. Sci. USA 94, 10249–10254.
[13] Akabas, M.H., Stauffer, D.A., Xu, M. and Karlin, A. (1992) Science 258, 307–310.
[14] Iwamoto, T., Wakabayashi, S., Imagawa, T. and Shigekawa, M. (1998) Eur. J. Cell Biol. 76, 228–236.
[15] Iwamoto, T. and Shigekawa, M. (1998) Am. J. Physiol. 275, C423–C430.
[16] Uehara, A., Iwamoto, T., Shigekawa, M. and Imanaga, I. (1997) Pfügers Arch. 434, 335–338.
[17] Haddock, P.S., Coetzee, W.A. and Artman, M. (1997) Am. J. Physiol. 273, H837–846.
[18] Fu, D., Ballesteros, J.A., Weinstein, H., Chen, J. and Javitch, J.A. (1996) Biochemistry 35, 11278–11285.
[19] Grunewald, M., Bendahan, A. and Kanner, B.I. (1998) Neuron 21, 623–632.
[20] MacKinnon, R. (1995) Neuron 14, 889–892.